August 1984

LBL--18301

DE85 000699

SIMULATING SUPERSYMMETRY AT THE SSC

A contribution to the Proceedings of the
1984 DPF Summer Study on the
Design and Utilization of the
Superconducting Super Collider.
June 23-July 13, 1984, at Snowmass, CO. 81611

R. Michael Barnett

Department of Physics
University of California
Santa Barbara, CA 93106
and
Lawrence Berkeley Laboratory
and
Department of Physics
University of California
Berkeley, CA 94720

and

Howard E. Haber

Department of Physics
University of California
Santa Cruz, CA 95064
and
Stanford Linear Accelerator Center
Stanford University
Stanford, CA 94305

This work was supported by the Director, Office of Energy Research, Office of High Energy and Nuclear Physics, Division of High Energy Physics of the U.S. Department of Energy under Contract DE-AC03-76SF00098, the U.S. National Science Foundation under Agreement No. PHY83-18358 and Grant No. PHY8115541, and by the U.S. Department of Energy under Contracts Nos. DE-AM03-76SF00010 and DE-AC03-76SF00515.

Simulating Supersymmetry at the SSC

R. Michael Barnett
Department of Physics, University of California, Santa Barbara, CA 93106
and
Lawrence Berkeley Laboratory, Berkeley, CA 94720
and
Howard E. Haber
Department of Physics, University of California, Santa Cruz, CA 95065
and
Stanford Linear Accelerator Center, Stanford University, Stanford, CA 94305

Summary

Careful study of supersymmetric signatures at the SSC is required in order to distinguish them from Standard Model physics backgrounds. To this end, we have created an efficient, accurate computer program which simulates supersymmetric particle production and decay (or other new particles). We have incorporated the full matrix elements, keeping track of the polarizations of all intermediate states. (At this time hadronization of final-state partons is ignored). Using Monte Carlo techniques this program can generate any desired final-state distribution or individual events for Lego plots. Examples of the results of our study of supersymmetry at SSC are provided.

We describe here a computer program which is designed to generate large numbers of simulated events appropriate for a high-energy machine (such as the superconducting Super Collider (SSC)). The program uses Monte-Carlo techniques to simulate events from pp or $p\bar{p}$ collisions. Using parton model formalism, we consider the large-p_T production via a hard-scattering process of heavy particles which subsequently decay. The output of our program consists of four-momenta of all final state particles in the laboratory center-of-mass. At present, we do not hadronize final-state quarks and gluons (as well as spectator hadronic constituents); therefore, we must interpret final-state quarks and gluons as hadronic jets. We plan to address this issue in the future.

At the Snowmass Summer Study, we have applied our program to the production of supersymmetric particles at the SSC. We studied the associated production of photinos ($\tilde{\gamma}$) and gluinos ($\tilde{g}$), and that of W-inos ($\tilde{W}$) and gluinos. With our program, we are able to obtain normalized total and differential cross-sections for supersymmetric particles production under simulated experimental conditions. Many distributions and scatterplots of final state variables can be studied. One can also study typical events on a one-by-one basis.

Before presenting some of our results, we begin with a description of the techniques used in the event-simulating computer program. The first task is to choose the momenta of the two colliding quarks (or gluons). The event is then weighted according to appropriate distribution functions (u(x), d(x), u(x), s(x), etc.). We used the distribution functions of Eichten, Hinchliffe, Lane, and Quigg[1] (EHLQ) with $\Lambda = 0.29$ GeV. Choosing x_1 and x_2 randomly would give mostly events with small weights (especially at SSC energies where the distribution functions peak sharply at small x). Instead we choose randomly the variables:

$$\eta \equiv \tfrac{1}{2}\ln x_1/x_2 \quad \text{between} \quad -\tfrac{1}{2}\ln s/\hat{s}_0 \text{ and } \tfrac{1}{2}\ln s/\hat{s}_0$$

$$\xi \equiv 1/(x_1 x_2) \quad \text{between} \quad \exp(2|\eta|) \text{ and } s/\hat{s}_0$$

where $\hat{s}_0 = (m_{\tilde{g}} + m_{\tilde{\gamma}})^2$. The weight must be multiplied by the additional factor $(s/\hat{s}_0 - 1)\ln(s/\hat{s}_0)/\xi^2$ when using these variables. These variables which were suggested to us by J. Gunion and M. Soldate make a much more efficient choice of x_1 and x_2.

With x_1 and x_2 chosen, the program can then calculate the incoming momentum vectors which are input to the phase-space integration routine "SAGE". The output of SAGE are the four-momenta of the outgoing particles plus a phase-space weight factor to be multiplied with the previous weight factors. These outgoing particles may in turn be decayed. Although the particles of concern to us are easily narrow enough to validate use of the narrow width approximation, SAGE also has an efficient Breit-Wigner routine allowing finite widths for decaying particles.

The final factor in the weight of each event is the full, squared matrix element which we describe later. We have kept all events but some have greater weights than others. A normalized cross-section is obtained simply by summing the weights, dividing by the number of events and multiplying by the appropriate flux factor. We have checked total cross-sections analytically and find our results to be very accurate with remarkably few events needed (about 1000 are adequate).

To simulate experimental conditions, we may eliminate events which fail to pass certain kinematical cuts in electron transverse momentum, missing energy, rapidity and/or other variables. For jets which are too close, we may coalesce them. The resulting distributions and scatterplots will then reflect these changes. By testing against a random number generator, we can choose typical events and examine them on Lego-type plots.

We now turn to some examples of supersymmetric processes. For the purposes of this study, we assume that the masses of all directly-produced supersymmetric particles are sufficiently heavy so that they could only be discovered at SSC energies. We take the photino to be the lightest supersymmetric particle; it interacts very weakly and, like neutrinos will always escape the detector.

One possible class of events which could be evidence for supersymmetry are "one-sided events", e.g. events with large-p_T hadronic jets in one hemisphere and no large-p_T jets in the opposite hemisphere (due to escaping photinos). An event of this type would be $pp \to \tilde{g}\tilde{\gamma} + X$. The gluino decays via $\tilde{g} \to q\bar{q}\tilde{\gamma}$ and can result in two large-p_T jets in one hemisphere with no recoiling jets in the opposite hemisphere.

The possible standard model backgrounds may be severe. For example, $pp \to gZ + X$, $Z \to \nu\bar{\nu}$ and $pp \to ZW + X$, $Z \to \nu\bar{\nu}$ and $W \to$ hadronic jets both yield one-sided events. The various Standard Model backgrounds need to be carefully studied in order to learn whether possible signals for new physics can be extracted from a sample of one-sided events.

A second class of events which could be a signal for supersymmetry are "two-sided events" with missing transverse energy. We shall focus on those two-sided events in which one hemisphere consists of large-p_T hadronic jets and the opposite hemisphere consists solely of an isolated electron (or muon). The supersymmetric process corresponding to this signal with the largest cross-section[1,2,3] may be $pp \to \tilde{W}\tilde{g} + X$. The signature of this process depends crucially on the supersymmetric mass spectrum. Two cases of interest are as follows: (a) If the W-ino, $\tilde{w}$, is the second lightest supersymmetric particle (the photino is assumed to be the lightest), then the dominant decay of the W-ino is $\tilde{w} \to W\tilde{\gamma}$. Since BR($W \to e$ or $\mu + \nu$) $\approx 16\%$, about one in every six $\tilde{w}\tilde{g}$ events would resemble the signature described above. (We neglect the τ's here). (b) If the only particles lighter than the $\tilde{w}$ are the scalar-neutrino ($\tilde{\nu}$) and photino, then the process $\tilde{w} \to \ell\tilde{\nu}$, ($\ell$ = e, ν, τ) must also be considered ; the $\tilde{\nu}$ decays via $\tilde{\nu} \to \nu + \tilde{\gamma}$ and is not observed. The Standard Model backgrounds to these events will come dominantly from $pp \to W^+W^- + X$ where one W decays leptonically and one W decays hadronically. It is a non-trivial problem to ascertain whether a wg signal as described above could be separated from such a background.

We shall use the two processes, $\tilde{g}\tilde{\gamma}$ and $\tilde{w}\tilde{g}$ to illustrate our procedure. In the case of $\tilde{g}\tilde{\gamma}$, the partonic subprocess is $q\bar{q} \to \tilde{g}\tilde{\gamma} \to q\bar{q}\tilde{\gamma}\tilde{\gamma}$. The full matrix element for $q\bar{q} \to q\bar{q}\tilde{\gamma}\tilde{\gamma}$ is obtained in the narrow resonance approximation: $\tilde{g} \to \tilde{q}\bar{q}$ or $\bar{\tilde{q}}q$, $\tilde{q} \to q\tilde{\gamma}$ where the $\tilde{g}$ width is taken to be small compared to its mass (which is a very good approximation here), and the scalar-quark $\tilde{q}$ can either be taken to be real or virtual. If $\tilde{q}$ is real, then the narrow-resonance approximation can also be used for its decay. We assume that the two types of scalar-quarks $\tilde{q}_L$ and $\tilde{q}_R$ are degenerate in mass. Then, the above process is parity invariant which implies that the outgoing $\tilde{g}$ and $\tilde{\gamma}$ are not longtudinally polarized. Furthermore, the tree diagrams $q\bar{q} \to q\bar{q}\tilde{\gamma}\tilde{\gamma}$ are real; hence the outgoing $\tilde{g}$ and $\tilde{\gamma}$ are not transversely polarized. The end result is that in the narrow-width approximation, the squared matrix element for $q\bar{q} \to q\bar{q}\tilde{\gamma}\tilde{\gamma}$ factorizes into the squared matrix elements for production[4] $q\bar{q} \to \tilde{g}\tilde{\gamma}$ and decay $\tilde{g} \to q\bar{q}\tilde{\gamma}$ respectively. Once we have the complete squared matrix element for $q\bar{q} \to q\bar{q}\tilde{\gamma}\tilde{\gamma}$, we may insert this into our program and generate events consisting of the four-momenta of the outgoing q, $\bar{q}$ and photinos in the pp center-of-mass frame.

In the case of $\tilde{w}\tilde{g}$, the partonic subprocess is $u\bar{d} \to \tilde{w}^+\tilde{g}$ (via $\tilde{d}_L$ and $\tilde{u}_L$ exchange) followed by the decays. (We also add in the charge conjugate process $\bar{u}d \to \tilde{w}^-\tilde{g}$.). The gluino decays via $\tilde{g} \to q\bar{q}\tilde{\gamma}$; we shall assume that the W-ino decays into $\tilde{w}^\pm \to e^\pm\tilde{\nu}$. The appropriate couplings are described in Refs. 4 and 5. In this case, the process is parity-violating so that the outgoing $\tilde{w}$ is (partially) longitudinally polarized. Therefore, even in the narrow-resonance approximation the squared matrix element for $u\bar{d} \to q\bar{q}e^+\tilde{\gamma}\tilde{\nu}$ does not factorize into the production and decay squared matrix elements. To properly keep track of the polarizations, one may compute the appropriate 2- to -5 tree-level Feynman diagrams, putting the intermediate $\tilde{w}$ and $\tilde{g}$ on-shell. The final expression may be found in Ref. 6. Note that if one wishes to study another decay mode of the $\tilde{w}$ such as $\tilde{w} \to W\tilde{\gamma}$, a new computation will be needed for the 2- to -6 process $u\bar{d} \to q\bar{q}e^+\nu\tilde{\gamma}\tilde{\gamma}$. Once the complete matrix element has been obtained, we may generate events consisting of the four-momenta of the final state particles.

In principle, the following steps are necessary at this point: final-state quarks (and gluons) must hadronize and hadronization of spectator partons (including initial state radiation) should be accounted for. There are a number of possible procedures in the literature; we are at present deciding how to incorporate this aspect into our program. In the meantime, we present results in which we simply interpret outgoing quarks and gluons as hadron jets. We expect this to be a crude approximation to the eventual output once hadronization has been included.

We shall display some results we have obtained for wg production. Since space is limited here and the results for $\tilde{\gamma}\tilde{g}$ often resemble those for $\tilde{w}\tilde{g}$ without the electron, we will show those results elsewhere. In Figs. 1 and 2 we have chosen $m(\tilde{w}) = m(\tilde{q}) = 950$ GeV and $m(\tilde{g}) = 1000$ GeV. Figure 1 shows dramatically that having similar $\tilde{q}$ and $\tilde{g}$ masses leads to one high-energy jet and one very low-energy jet. The electron transverse momentum coincides with the high-energy jet (so is not shown) whereas the missing transverse energy peaks at higher energies. The angle between jets is in general quite large, so there will be no trouble separating them. For contrast we show similar plots in Figs. 3 and 4 for $m(\tilde{q}) = 500$ GeV, $m(\tilde{w}) = 950$ GeV and $m(\tilde{g}) = 1000$ GeV.

In conclusion, we have demonstrated that our program can produced valuable results quickly and efficiently. Only a sample are shown here. Further studies with this program may lead to an improved understanding of our ability to separate these new physics signals from backgrounds at the SSC.

Acknowledgments

We acknowledge valuable discussions with S. Dawson, E. Eichten, J. Gunion, I. Hinchliffe, G. Kane, F. Paige, A. Savoy-Navarro, and M. Soldate. This work was supported by the Director, Office of Energy Research, Office of High Energy and Nuclear Physics, Division of High Energy Physics of the U.S. Department of Energy under Contract DE-AC03-76SF00098, the U.S. National Science Foundation under Agreement No. PHY83-18358 and Grant No. PHY8115541, and by the U.S. Department of Energy under Contracts Nos. DE-AM03-76SF00010 and DE-AC03-76SF00515.

References

1. E. Eichten et al., report no. FERMILAB-Pub-84/17-T.

2. H. E. Haber and G. L. Kane, *Phys. Lett.* 142B, 212 (1984).

3. S. Dawson, E. Eichten and C. Quigg, report no. FERMILAB-Pub-83/82-THY.

4. R. M. Barnett and H. E. Haber, report no. NSF-ITP-84-78 (1984).

5. For a recent review and a complete set of references, see: H. E. Haber and G. L. Kane, report no. UM HE TH 83-17 (1984), to be published in *Phys. Rep.*

6. R. M. Barnett, H. E. Haber and G. L. Kane, report (in progress).

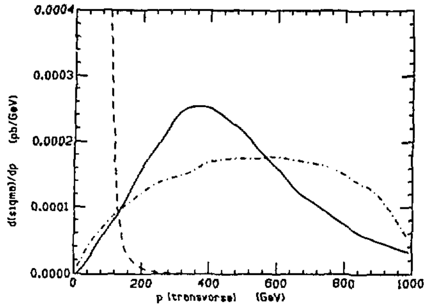

Figure 1. The distributions from $\tilde{w}\tilde{g}$ production of transverse momentum for the fast jet (solid), the slow jet (dashed) and the electron (indistinguishable from solid curve). The dot-dash curve is the missing transverse energy. $M(\tilde{w}) = m(\tilde{q}) = 950$ GeV and $m(\tilde{g}) = 1000$ GeV.

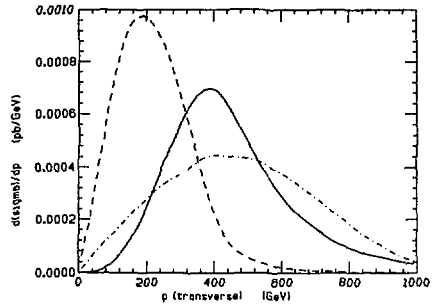

Figure 3. The distributions from $\tilde{w}\tilde{g}$ production of transverse momentum for the fast jet (solid) and the slow jet (dashed). The dot-dash curve is the missing transverse energy. $m(\tilde{w}) = 950$ GeV, $m(\tilde{q}) = 500$ GeV and $m(\tilde{g}) = 1000$ GeV.

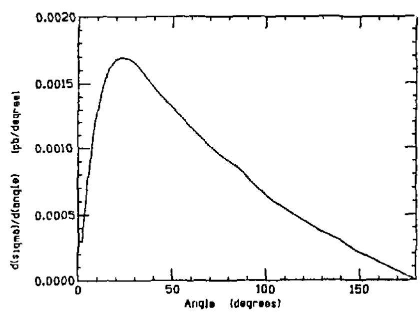

Figure 2. The angle between the two jets. Masses as in Fig 1.

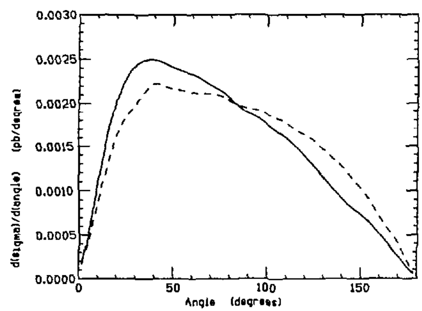

Figure 4. The angles between the two jets (solid) and between the fast jet and the electron. Masses as in Fig. 3.